Electronic Supplementary Material (ESI) for New Journal of Chemistry.
This journal is © The Royal Society of Chemistry and the Centre National de la Recherche Scientifique 2024

Supporting Information for

Decoding the ICT-PET-ESIPT Liaison Mechanism in a Phthalimide-based Trivalent Transition Metal Ions Specific Chromo-fluorogenic Probe

Sabbir Ahamed[a], Manas Mahato[a], Rajkumar Sahoo[b], Najmin Tohora[a], Tuhina Sultana[a], Arpita Maiti[a] and Sudhir Kumar Das[a]*

[a]Department of Chemistry, University of North Bengal, Darjeeling, West Bengal 734013, India

[b]Department of Chemistry, Indian Institute of Technology, Kharagpur-721302, India

Corresponding author: (Dr. S. K. Das; E-mail: sudhirkumardas@nbu.ac.in)

Table of contents

1. Synthetic procedure of HBAI

For the synthesis of salicylimine-based Salen derivative, **HBAI** (**Scheme 1**), 4-aminophthalimide is dissolved in 2 ml of methanol and then we added 1 equivalent of salicylaldehyde dropwise to the solution with a catalytic amount of acetic acid. The mixture is refluxed at 60 ℃ for six hours. Then, the solution is furnished to a golden yellow precipitation and allowed to cool at room temperature. Then the precipitation is filtered off and washed several times with hot methanol. Yield = 87 %.

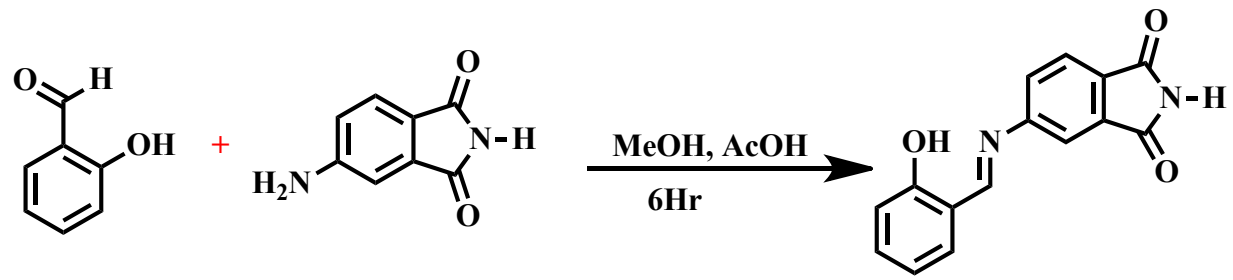

Scheme 1. Synthetic route for the preparation of **HBAI.**

2. Materials and instruments

Phthalimide, other reagents, and every metal cationic perchloride salt were purchased from the commercial supplier and used without purification. All the solvents are used for the preparation and spectroscopic analysis purposes in HPCL grade. ^{1}H NMR and ^{1}H NMR titration experiments are carried out on a Bruker 400 MHz instrument with chemical shifts (δ) in ppm unit. The same system is also used for the ^{13}C NMR spectra measured with a frequency of 100 MHz. High-resolution mass spectra (HRMS) have been carried out on an Agilent 6545XT Advance-Bio LC/Q-TOF spectrometer. UV-visible spectroscopic analyses are carried out in HITACHI U-2910. Photoluminescence experiments are carried out using HITACHI F-7100 fluorimeter with 10 nm excitation and emission slit, respectively, under room temperature. Emission and excitation wavelength at the time of the fluorescent experiment were controlled at 400nm and 420 nm, respectively.

3. Measurement of fluorescence quantum yield

For the estimation of fluorescence quantum yield, we have considered the 4-aminophthalimide (4-AP) as a standard in DMSO (Φ=0.83). Using the equation $: \Phi = \Phi_s\left(\frac{F_x}{F_s}\right)\left(\frac{A_s}{A_x}\right)\left(\frac{{\eta_x}^2}{{\eta_s}^2}\right)$, where Φ stands for quantum yield, F is the integrated fluorescence intensity, A is the absorbance, η defines the refractive index of the solvent, subscript 's' represents the standard 4-AP, and x is the unknown one. We have calculated the quantum yield (Φ) of our sensor **DAID** and **DAID**-Al^{3+} complex as 0.0038 and 0.37, respectively.

3. Measurement of fluorescence lifetime decay profiles

The time-resolved fluorescence lifetime decay profiles are recorded by a picosecond time-correlated single photon counting (TCSPC) system (LifeSpec II, Edinburgh Instruments, U.K.) with the help of 375 nm pulsed laser source having pulse width 68 ps. The emissions signals are collected at the corresponding emission maxima by using a photomultiplier tube (H10720-01, Hama matsu) at magic angle 54.7°. For the determination of instrument response function (IRF) a colloidal Ludox solution is used which is found to be 270 ps. After deconvoluting the IRF, each decay curve is fitted by using an exponential decay function utilizing the equation: $\tau(t) = \Sigma b_i e^{-t/\tau_i}$ having goodness of fit (χ^2) values near to unity. Here, in the equation α_i and τ_i are the experimentally obtained pre-exponential factors and its corresponding lifetimes. Experimentally obtained pre-exponential factors are normalized by the equations $\alpha_i = \frac{b_i}{\Sigma b_i}$ to achieve actual pre-exponential factors which is multiplied by 100 to obtained percentage of molecules corresponding to each lifetime. The average fluorescence lifetime are estimated with help of equation: $<\tau> =$

$\frac{\Sigma \alpha_i \tau_i}{\Sigma \alpha_i}$. The photoluminescence decay behaviour of **HBAI** and **DAID** are found to be bi and tri-exponential in nature.

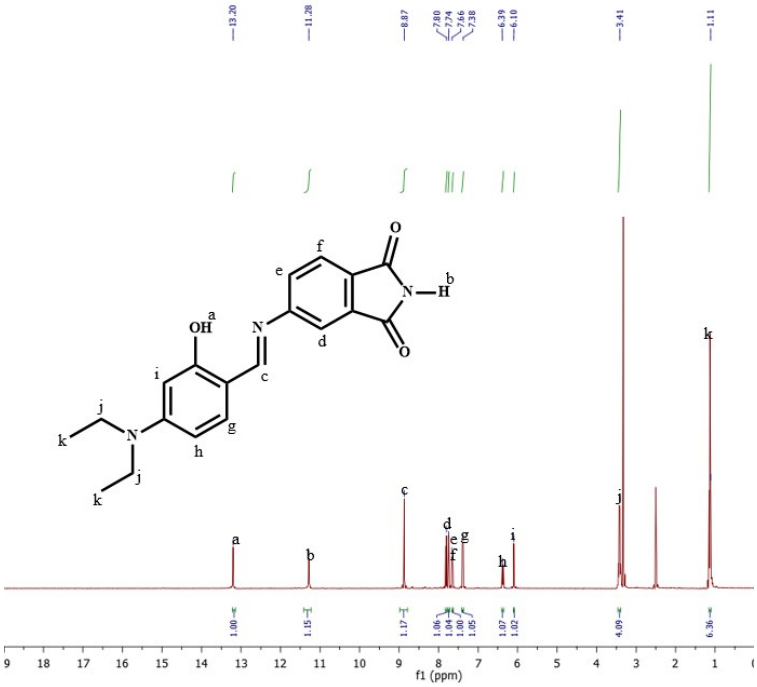

Fig. S1: [1]H NMR spectrum of our prepared probe **DAID** in DMSO-d_6.

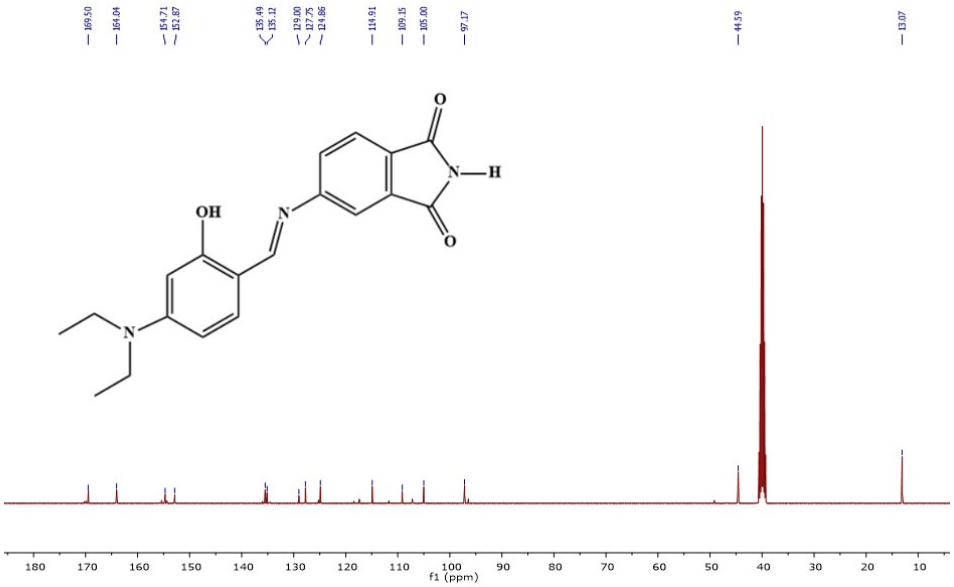

Fig. S2: [13]C-NMR spectra of our synthesized **DAID**.

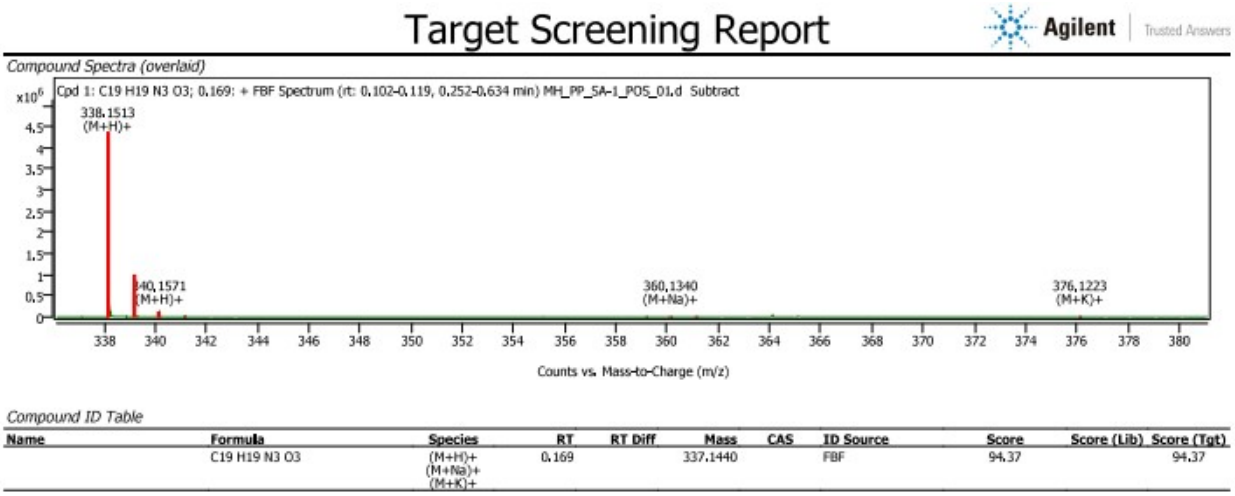

Fig. S3: High-resolution mass spectra of our synthesized **DAID**

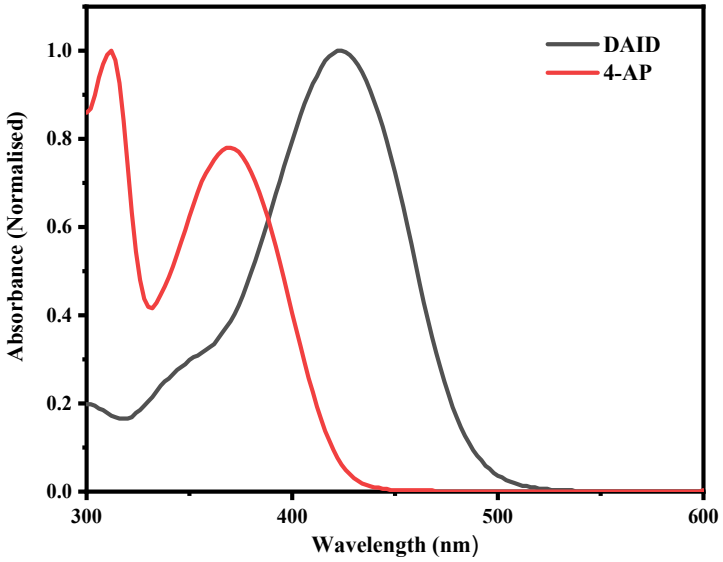

Fig. S4: Normalization plot of UV-visible titration spectra of **DAID** and the parent moiety of 4-AP.

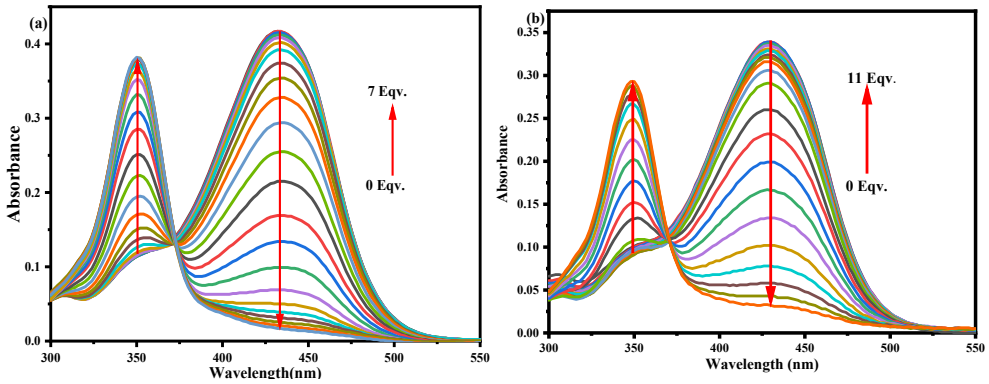

Fig. S5: (a) & **(b)** UV-visible absorption titration spectra of **DAID** upon gradual addition of Cr^{3+} (0 - 7 equiv.) and Fe^{3+} (0 - 11 equiv.) in 20% water-DMSO mixture.

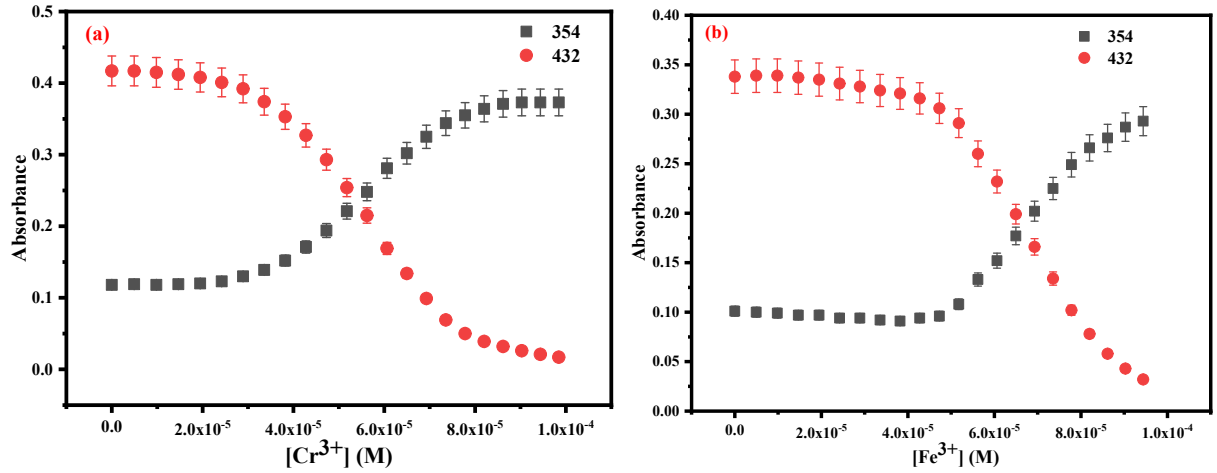

Fig S6: (a) & **(b)** Change of absorbance values with the addition of (M^{3+} = Cr^{3+} and Fe^{3+}) at wavelengths 354 nm & 432 nm and 348 nm & 430 nm respectively in 20% (v/v) water-DMSO mixture.

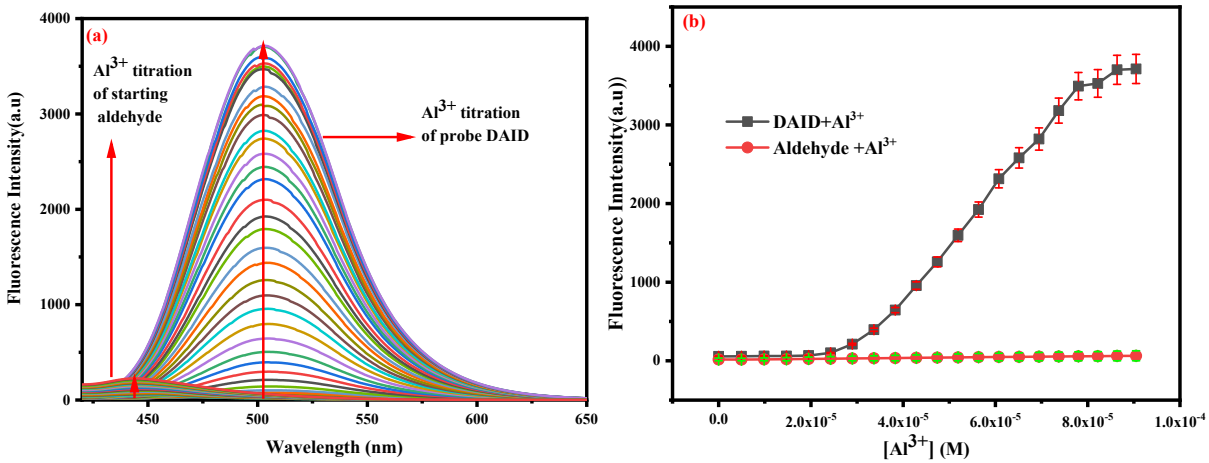

Fig S7: (a) Combine emission titration spectra of **DAID** with parent aldehyde moiety upon gradual addition of Al^{3+} ions. **(b)** Comparison of emission intensity between **DAID** and parent aldehyde moiety within the equimolar addition of Al^{3+} ions.

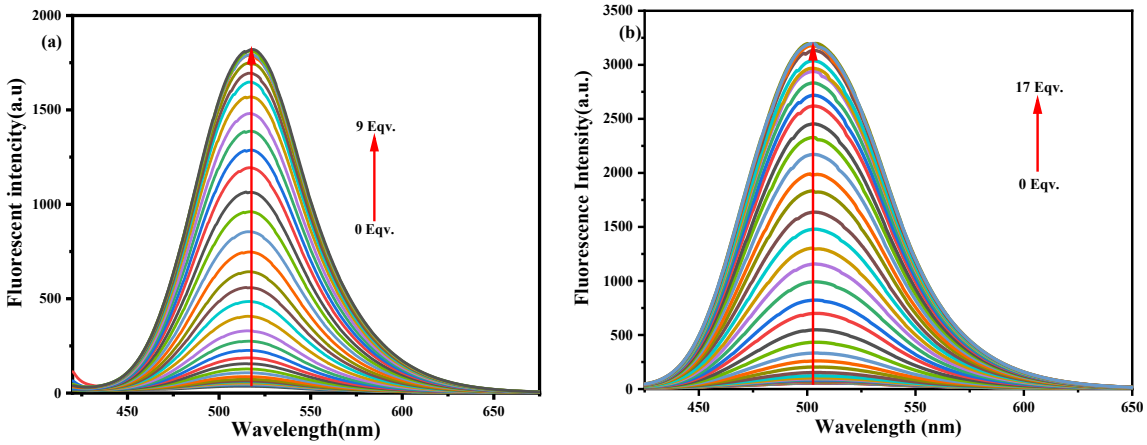

Fig. S8: (a) & **(b)** Emission titration spectra of **DAID** upon gradual addition of Cr^{3+} and Fe^{3+} (0 equiv. 9 equiv.) and (0 to 17 equiv.) in 20% water-DMSO mixture.

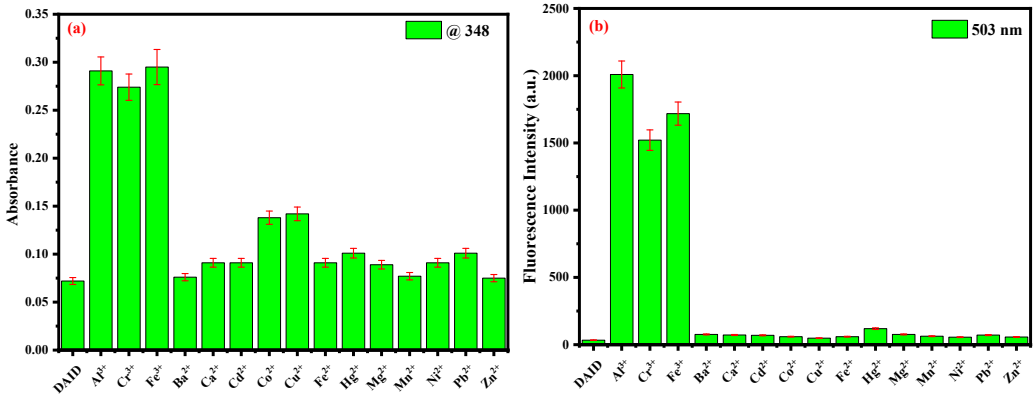

Fig. S9: (a) & **(b)** Metal selectivity bar diagram demonstration concerning absorbance values and Fluorescence intensity respectively.

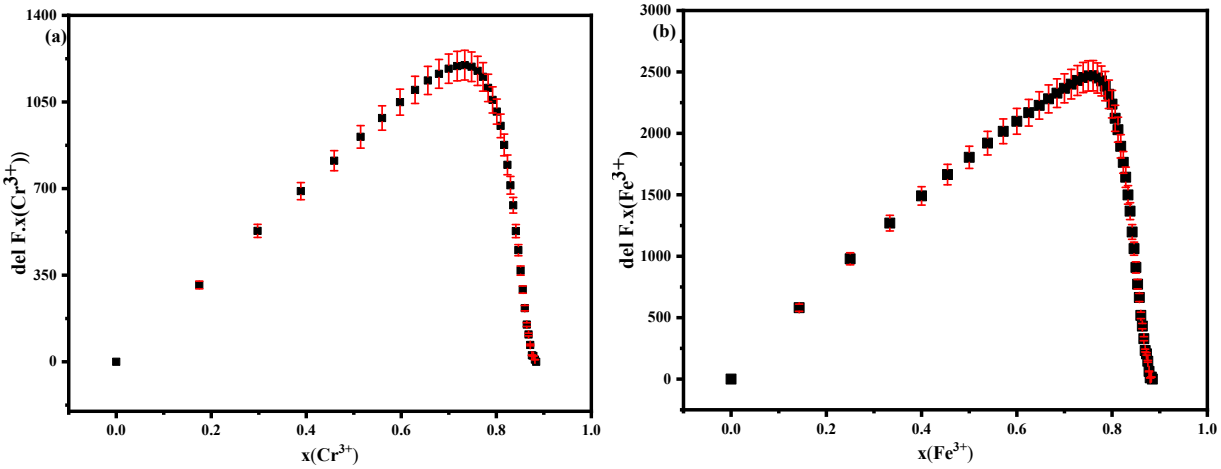

Fig. S10: (a) & **(b)** Job's plot of **DAID** with the addition of Cr^{3+} and Fe^{3+} ions in 20% H_2O – DMSO mixture to determine stoichiometric relation, respectively.

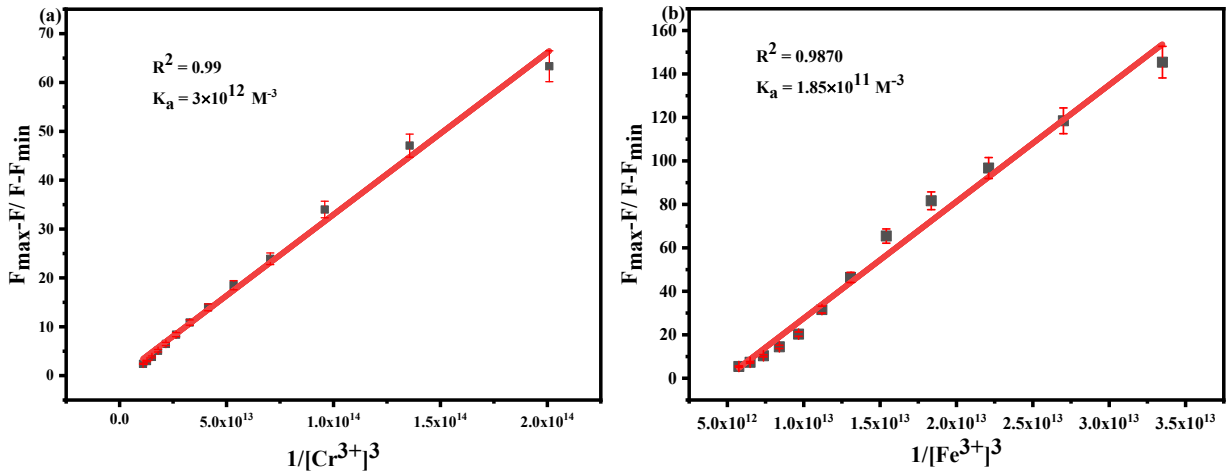

Fig. S11: (a) & **(b)** Benesi-Hildebrand plot fitting in **DAID**-Cr^{3+} and Fe^{3+} complex for the estimation of binding constant.

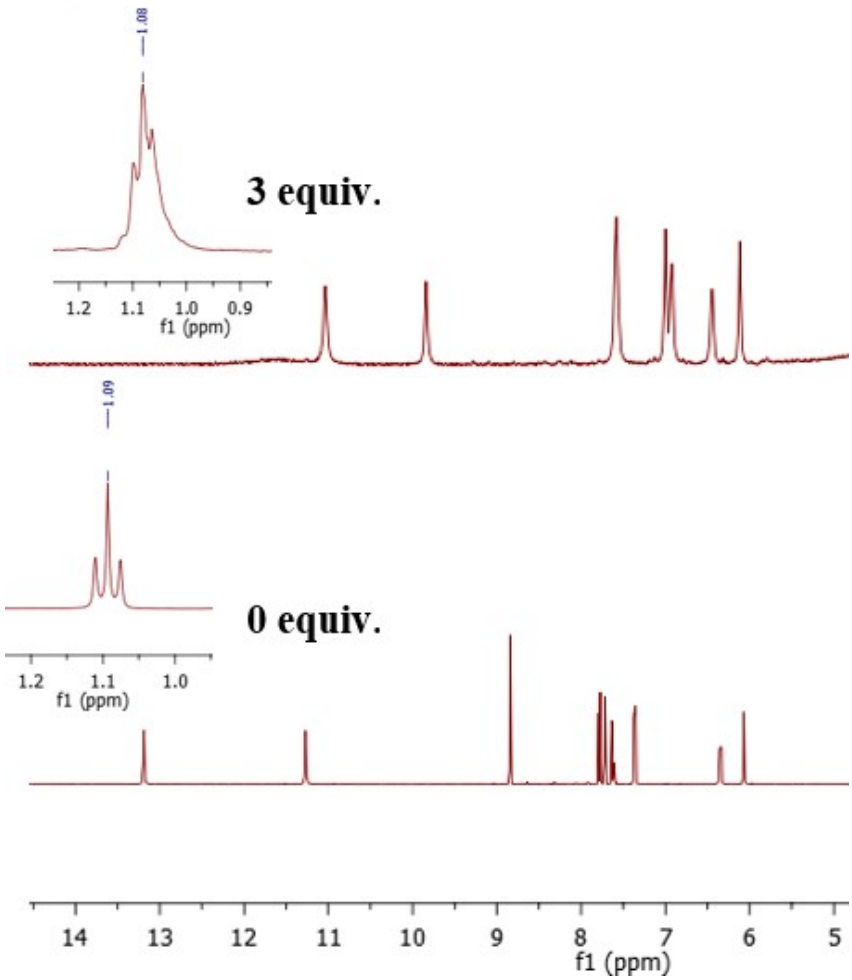

Fig. S12: Partial ^{1}H – NMR titration spectra of **DAID** due to the addition of Al^{3+} ions. The inset figure indicates the shifting of ethyl proton from 1.09 to 1.08 ppm.

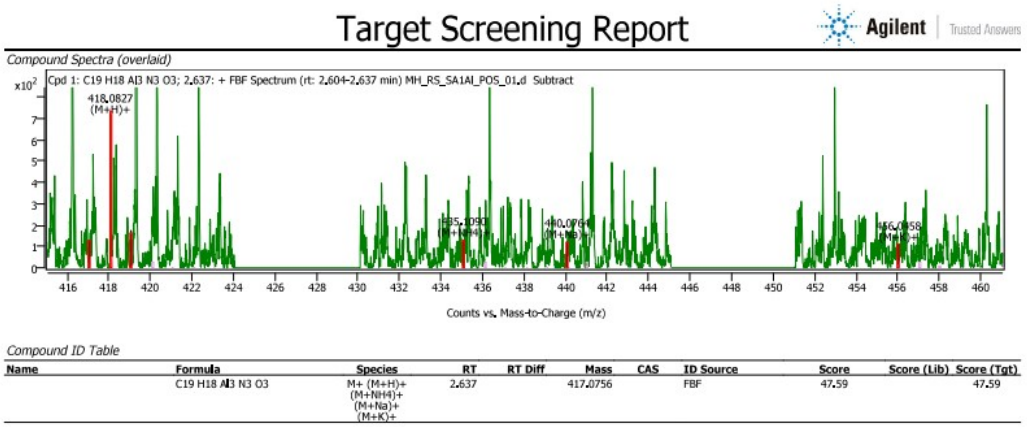

Fig. S13: High-resolution mass spectra of **DAID** – Al^{3+} complex (m/z) 418.0827.

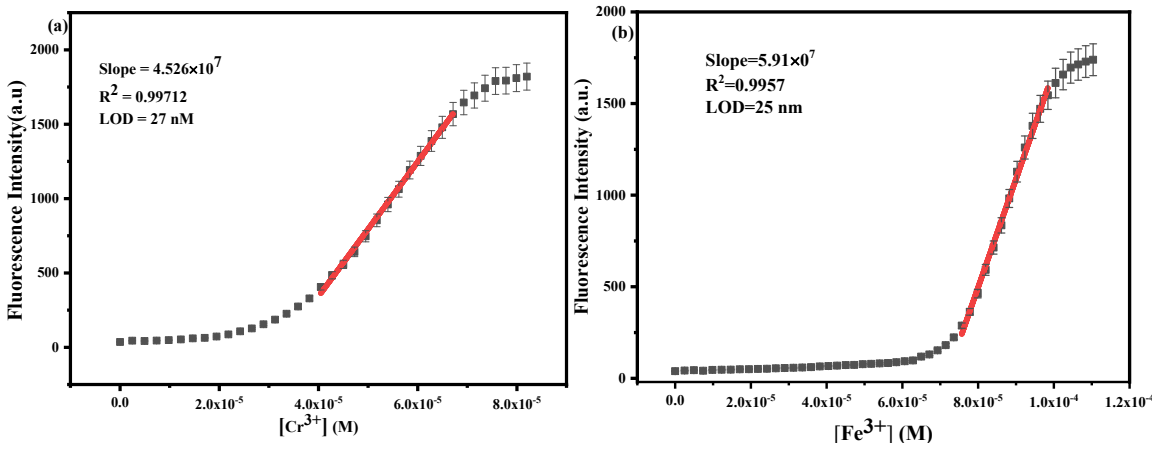

Fig. S14: (a) & **(b)** The linear response curve of emission intensity for determination of detection limit for Cr^{3+} and Fe^{3+} in 20% water-DMSO mixture.

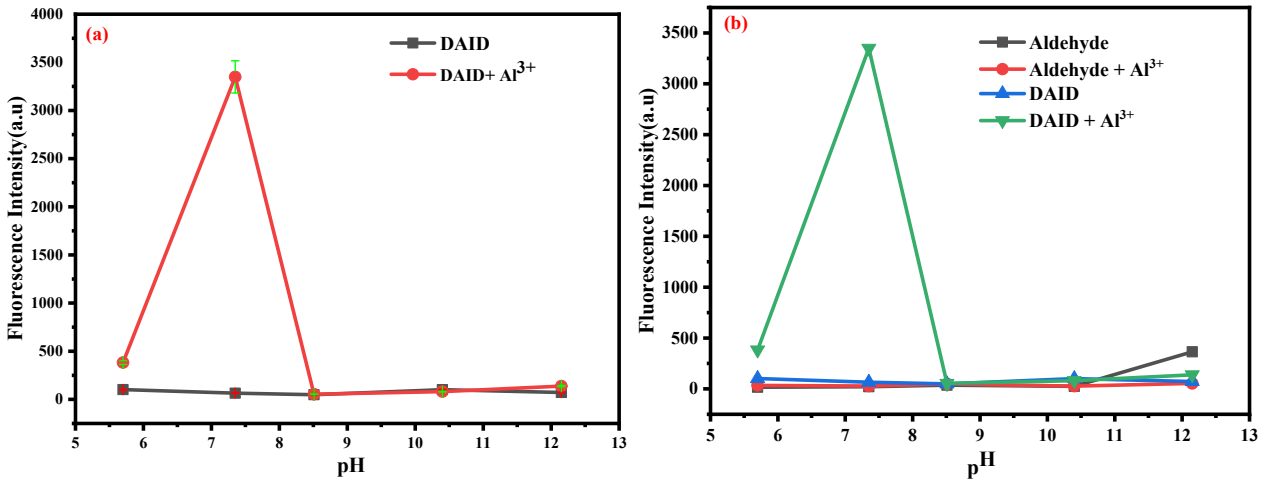

Fig. S15: (a) Fluorescence intensity of **DAID** and its stable complex **DAID**-Al^{3+} in pH 5-12. **(b)** Comparison of emission intensity between **DAID**, parent aldehyde moiety, and their Al^{3+} complex within pH 5-12

Table S1: Comparison table of chemosensors that have been introduced to detect trivalent metal cations in the last few decades with our probe DAID.

Probe	Solvent	λ_{ex} (λ_{em})/ nm	LOD	K_a	Ref no.
1	Pure CH_3CN	437 (475)	0.5 μM (Cr^{3+}) 0.3 μM (Al^{3+}) 0.2 μM (Fe^{3+})	1.58×10^4 M^{-1} (Cr3+); 6.46×10^9 M^{-2} (Al^{3+}); 1.26×10^5 M^{-1} (Fe3+);	1
2	CH_3CN–HEPES buffer solution (40/60, v/v, pH = 7.4)	342 (484)	25 μM (Cr^{3+}) 23 μM (Al^{3+}) 20 μM (Fe^{3+})	1.08×10^4 M^{-1} (Fe^{3+}); 8.77×10^3 M^{-1} (Al^{3+}) 5.68×10^3 M^{-1} (Cr^{3+})	2
3	CH_3CN–HEPES buffer solution (1:1), pH = 7.4)	460 (675)	93 nM (Cr^{3+}) 32 nM (Al^{3+}) 90 nM (Fe^{3+})	Not determined	3
4	H_2O:EtOH (8:2)	390 (563) 390 (527)	0.20 μM (Cr^{3+}) 0.50 μM (Al^{3+})	5.50×10^4 M^{-1} (Cr^{3+}); 2.00×10^4 M^{-1} (Al^{3+});	4
5	CH_3OH–H_2O (6 : 4), (v/v)	330 (582)	1.74 μM (Al^{3+}); 2.36 μM (Cr^{3+}); 2.90 μM (Fe^{3+})	1.00×104 M^{-1} (Al^{3+}); 2.60×102 M^{-1} (Cr^{3+}) 1.20×102 M^{-1} (Fe^{3+});	5
6	H2O: MeOH (1: 1) mixture.	510 (555)	0.31 μM (Cr^{3+}); 0.34 μM (Al^{3+}); 0.29 μM (Fe^{3+})	6.00×10^4 M^{-1} (Cr^{3+}) 6.70×10^4 M^{-1} (Fe^{3+}); 8.20×10^4 M^{-1} (Al^{3+});	6
7	DMF/H_2O (v/v=1:1)	365 (501)	0. 337 μM (Cr^{3+}) 0. 358× μM (Fe^{3+}); 0.4.89 μM (Al^{3+})	2.06×10^6 M^{-1} (Cr^{3+}) 4.72×10^6 M^{-1} (Fe^{3+}) 1.85×10^7 M^{-1} (Al^{3+})	7
8	Pure MeOH	360 (583)	0.63 μM (Cr^{3+}); 0.14 μM (Fe^{3+}); 0.22 μM (Al^{3+})	0.87×10^4 M^{-1}(Cr^{3+}) 1.14×10^4 M^{-1}(Fe^{3+}) 4.48×10^4 M^{-1}(Al^{3+})	8
9	**20% (v/v) water-DMSO mixture**	**400 (503)**	**18.5 nM (Al^{3+})** **25 nM (Fe^{3+})** **27 nM (Cr^{3+})**	**4.30×10^{12} M^{-3} (Al^{3+})** **1.85×10^{11} M^{-3} (Fe^{3+})** **3.00×10^{12} M^{-3} (Cr^{3+})**	**In this work**

Reference

1 A. Barba-Bon, A. M. Costero, S. Gil, M. Parra, J. Soto, R. Martínez-Máñez and F. Sancenón, A new selective fluorogenic probe for trivalent cations, *Chem. Commun.*, 2012, **48**, 3000–3002.

2 S. Goswami, K. Aich, A. K. Das, A. Manna and S. Das, A naphthalimide– quinoline based probe for selective, fluorescence ratiometric sensing of trivalent ions, *RSC Adv.*, 2013, **3**, 2412–2416.

3 S. Goswami, K. Aich, S. Das, A. K. Das, D. Sarkar, S. Panja, T. K. Mondal and S. Mukhopadhyay, A red fluorescence ' off–on ' molecular switch for selective detection of Al^{3+}, Fe^{3+} and Cr^{3+} : experimental and theoretical studies along with living cell imaging, *Chem. Commun.*, 2013, **49**, 10739–10741.

4 J. Wang, Y. Li, N. G. Patel, G. Zhang, D. Zhou, and Y. Pang, A single molecular probe for multi-analyte (Cr^{3+}, $Al^{3+,}$ and Fe^{3+}) detection in aqueous medium and its biological application, *Chem. Commun.*, 2014, **50**, 12258–12261.

5 X. Chen, X. Y. Shen, E. Guan, Y. Liu, A. Qin, J. Z. Sun and B. Zhong Tang, A pyridinyl-functionalized tetraphenylethylene fluorogen for specific sensing of trivalent cations, *Chem. Commun.*, 2013, **49**, 1503–1505.

6 R. Alam, R. Bhowmick, A. S. M. Islam, A. Katarkar, K. Chaudhuri and M. Ali, A rhodamine based fluorescent trivalent sensor (Fe^{3+}, Al^{3+}, Cr^{3+}) with potential applications for live cell imaging and combinational logic circuits and memory devices, *New J. Chem.*, 2017, **41**, 8359–8369.

7 M. Zhang, L. Gong, C. Sun, W. Li, Z. Chang, and D. Qi, A new fluorescent-colorimetric chemosensor based on a Schiff base for detecting Cr^{3+}, Cu^{2+}, Fe^{3+} and Al^{3+} ions, *Spectrochim. Acta Part A Mol. Biomol. Spectrosc.*, 2019, **214**, 7–13.

8 X. Li Yue, C. Rui Li, and Z. Yin Yang, A novel colorimetric and fluorescent probe for trivalent cations based on rhodamine B derivative, *J. Photochem. Photobiol. A Chem.*,

2018, **351**, 1–7.